Atomic origin of hysteresis during cyclic loading of Si due to bond rearrangements at the crack surfaces

Robin L. Hayes
Department of Chemistry, New York University, New York, New York 10003-6688

Emily A. Carter[a)]
Department of Mechanical and Aerospace Engineering and Program in Applied and Computational Mathematics, D404A Engineering Quadrangle, Princeton, New Jersey 08544-5263

(Received 8 August 2005; accepted 20 October 2005; published online 27 December 2005)

The atomistic origin of fatigue failure in micron-sized silicon devices is not fully understood. Two series of density-functional theory calculations on cubic diamond Si explore the effect of surface bond formation on crack healing in systems which exhibit strong surface reconstruction. Both series introduce a separation between Si(100) layers (i.e., the crack) and allow the ions to relax to their minimum-energy configuration. The initial surface ionic positions are either bulk terminated or 2×1 reconstructed. A plot of the energy versus the introduced separation reveals that once the surfaces reconstruct, the crack is no longer able to return to the equilibrium configuration. Rather, the healed crack interface contains defects which places the flawed energy minimum at a finite strain of 3% and an increased energy of 1.13 J/m^2 relative to the equilibrium configuration. The irreversible plastic deformation supports the mechanism proposed by Kahn *et al.* [Science **298** 1215 (2002)] that invokes mechanically induced subcritical cracking to explain the delayed onset of failure. © *2005 American Institute of Physics*. [DOI: 10.1063/1.2137692]

I. INTRODUCTION

Microelectromechanical systems (MEMS) are often composed of silicon because of its unique electronic properties and the availability of preexisting manufacturing techniques and infrastructure. Given the technological importance of silicon devices, understanding the atomistic mechanisms which lead to their failure is important both economically as well as scientifically. Until 1992, it was assumed that dynamic crack formation or fatigue cracking, in which cracks form during cyclic loading at a lower peak stress than would be required to form a crack during monotonic loading, would not occur in silicon because it is a brittle material. Contrary to the expectations, Connally and Brown discovered that prenotched micron-sized samples fail when subjected to cyclic loading under humid conditions.[1] Subsequently, several groups have confirmed that both micron-sized samples of single-crystal and polycrystalline silicon undergo fatigue failure.[2–4] However, a recent experiment calls into question these studies by observing similar cracking behavior in both cyclic- and monotonic-loaded micromachined silicons.[5] Kahn *et al.*[6] has compiled and summarized the main experimental observations of silicon fatigue failure as follows: (1) morphological changes in areas of high stress, including surface roughening and oxide thickening, (2) a decrease in high cycle fatigue lifetime when the peak stress is increased, (3) a decrease in low cycle fatigue lifetime when R, the ratio between minimum and maximum stress (negative values denote compression), is decreased, (4) a decrease in fatigue lifetime associated with a larger initial flaw, which is assumed to be caused by subcritical crack growth, (5) no dependence on vacuum or air in fatigue lifetime for low cycle failure, but a significant decrease in lifetime during high cycle fatigue if water is present, and (6) a fatigue lifetime that depends only on the number of cycles, not the elapsed time or the test frequency.

Three mechanisms have been proposed to explain the phenomena of silicon fatigue cracking: stress-assisted surface oxide dissolution,[2] reaction layer fatigue,[3] and mechanically induced subcritical cracking.[4] Stress-assisted surface oxide dissolution assumes that oxide forms on the freshly exposed crack surfaces during the loading, but dissolves preferentially under high stress states, leading to deep grooves which serve to nucleate the catastrophic crack once the oxide reaches a critical thickness of 60 nm. The second theory starts from a similar premise; namely, that the amorphous oxide formation is promoted in regions of high stress such as the crack tip. However, in this model, microcracks form solely in the oxide via stress corrosion cracking. Catastrophic failure occurs once the crack reaches a critical size. The third and most recently proposed failure mechanism assumes that microcracking occurs in the silicon, not the silicon oxide layer. The accumulation of damage at the crack tip from subcritical crack growth during cycling eventually leads to fatigue failure. Oxidation only plays a tangential role by concentrating the stress in the crack tip region due to wedging effects.

Each of these theories rely upon processes that have not yet been conclusively verified. The first two models require a mechanism for either oxide dissolution or stress corrosion cracking, respectively, that is active during cyclic loading but not monotonic loading, and that depends only on the number

[a)]Electronic mail: eac@princeton.edu

of cycles, not the elapsed time. Similarly, the last model requires a mechanism to form irreversible damage at the crack tip during fatigue cycling.

Direct experimental observation of oxide formation as a function of stress is difficult. One experiment quantified the adsorption and subsequent dissociation of water on silicon surfaces.[7] Other experiments indirectly detect the influence of stress by measuring the oxide thickness in the crack tip region, often in postmortem studies.[2,3] Large-scale hybrid quantum-mechanical/empirical potential simulations[8,9] predict that the dissociation of water molecules in a crack tip region under tension is barrierless. In contrast, *ab initio* simulation of water interacting with a strained silicon cluster found no evidence for enhanced chemical reactivity.[10] A separate large-scale empirical potential molecular-dynamics simulation showed that the void growth in front of the crack in amorphous silica eventually leads to failure.[11] However, these simulations have not been extended to include the complete stress corrosion cracking cycle. There has been no atomistic simulation that shows how stress-enhanced oxide dissolution occurs. Contrary to the previous results, two experiments have found that stress corrosion cracking did not play a significant role during dynamic fracture in silicon, although subcritical crack growth may have had a limited role.[6,12]

There are conflicting results for crack healing in silicon as well. A transmission electron microscopy (TEM) study in 1980 clearly demonstrated that cracks can heal imperfectly in bulk brittle materials such as Si, Ge, and Al_2O_3.[13] More recent experiments based on luminescence measurements during the cracking in thin Si wafers claim that fracture surfaces can heal perfectly, although direct imaging of the healed crack interface is not provided.[14,15] The difference may be related to how fast defects can be annealed away. One measure of the minimum annealing time is the recombination time of vacancy interstitial pairs. A molecular-dynamics simulation estimated that vacancy interstitial pairs only require microseconds, rather than the minutes previously estimated, to overcome the recombination barrier at room temperature, indicating that defects may anneal away at higher temperatures or longer times.[16] Another experiment found that a crack annealed in oxygen exhibited increased strength, but a crack annealed in vacuum did not. The increased strength in the former case was attributed to the formation of an oxide layer that healed the crack,[17] while the lack of increased strength in the latter suggests that defects may remain despite annealing.

It is also known that the crystal structure and chemical bonding can have a profound effect on crack behavior. Hybrid first-principles/empirical potential simulations of fracture in silicon show that the discrete nature of bond breaking at the crack tip produces lattice trapping, resulting in metastable crack surfaces and anisotropy in the fracture direction. These effects ultimately modify the crack morphology by modifying the brittle to ductile transition and cracking direction.[18–21] Given the complicated competing interactions among surface chemistry, the local stress state, and the local crystal structure, we choose to focus on the interface that forms between healed fracture surfaces as a potential mechanism for the formation of defects at the crack tip. This paper discusses first-principles density-functional theory (DFT) calculations, which suggest that surface reconstruction can cause an accumulation of damage at the crack tip which may lead to hysteresis during fatigue cycling of systems such as cubic diamond Si.

TABLE I. Physical properties of bulk diamond silicon and the Si(100)–2 $\times$1 surface. A_{eq} is the equilibrium lattice constant, B is the bulk modulus, C is the uniaxial elastic modulus given by $C=(1/d)C_{ijkl}m_i m_j m_k m_l$, where C_{ijkl} are the elastic constants (In the harmonic approximation, C_{ijkl} is calculated from $E(\varepsilon)=E(0)+V\frac{1}{2}\Sigma_{ijkl}C_{ijkl}\varepsilon_{ij}\varepsilon_{kl}$, where ε is the strain tensor, E is the total energy as a function of strain, and V is the volume.), **m** is the unit normal to cleavage plane and d is the interlayer spacing, γ_r is the energy of the reconstructed surface, d_{12} is the buckled dimer bond length, and the tilt angle is the inclination of the surface dimer relative to the flat surface. KSDFT is the current work.

Method	A_{eq} (Å)	B (GPa)	C (GPa/Å)	γ_r (J/m^2)	d_{12} (Å)	Tilt angle (deg)
KSDFT	5.460	87.9	101.5	1.32	2.30	17.4
Expt.	5.43[a]	100[b]	123.5[c]	1.36[d]	2.28±0.08[a]	19±2[a]

[a]Reference 30.
[b]Reference 32.
[c]Reference 33.
[d]Reference 34.

II. MODEL AND CALCULATIONAL DETAILS

We use a three-dimensional (3D) periodic generalized gradient approximation[22] (PW91) Kohn-Sham pseudopotential density-functional theory (KSDFT) calculations implemented within the VASP code.[23] Careful convergence tests using an ultrasoft pseudopotential established a kinetic-energy cutoff of 200 eV, an augmentation charge cutoff of 241.9 eV, and a Monkhorst-Pack k-point grid of $4\times8\times1$. These numerical parameters yield total energies converged to ~4 meV/atom. An atomic force criterion of 5 meV/Å was employed to ensure that the atomic relaxations were converged. 12 layers of Si were sufficient to insure that the results did not change upon the addition of extra layers. The physical properties of Si within our model, as listed in Table I, compare favorably with experimental values.

The use of 3D periodic KSDFT necessitates two simplifying approximations. First, instead of modeling a pointed crack tip, the crack is represented by two planes separated by a finite amount of vacuum. Essentially, this gives an average value of the material properties as a function of crack width. Second, the structurally well-characterized (100) surface is used instead of either the (111) or (110) surface, which are known to be the preferred crack surfaces.[24] Unfortunately, the (110) surface structure is not well-characterized experimentally and the size of the (111)-7$\times$7 surface reconstruction make calculations of (111) cleavage prohibitively expensive. Several types of atomic movement are at play at the crack region during fatigue cycling. One universal feature, regardless of the surface, is the breaking and formation of highly directional bonds near the crack tip. For Si(100)-2 $\times$1, a small displacement of surface atoms allow dimers to form, for Si(111)-7$\times$7, longer-range adatom migration is necessary for the full reconstruction. During fatigue cycling,

time is of the essence. The final crack surface structure is clear, but how it is achieved when the time available for atomic migration occurs in small segments is not obvious. Car-Parrinello molecular-dynamics simulations have shown that the Si(100)-2×1 reconstruction can form within 2 ps at room temperature,[25] indicating that bond formation and small atomic displacements should have enough time to form during typical cycling frequencies (1–$50\,000\ s^{-1}$). By contrast, a scanning tunneling microscopy (STM) study revealed that the Si(111)-7×7 surface reconstruction proceeds by the rapid nucleation of dimer-adatom stacking fault domains that subsequently coalescence into the full 7×7 surface on the order of minutes at room temperature and above.[26] Therefore, the full 7×7 reconstruction may not form immediately during the fatigue cycling, at least in the region near the crack tip. Furthermore, since the maximum applied cyclic load is lower than the load required to statically form cracks, crack extension during each fatigue cycle likely involves only a few atoms near the crack tip. Taken together, these imply that at least initially the dominant effect should simply be the localized breaking/forming of Si–Si bonds. Surface dimers in Si(100)-2×1 form bonds that must be broken if the perfect bulk cubic diamond structure is to be reformed. Consequently, our model captures the simplest, nontrivial example of the effect of surface bond formation on crack healing. For a moderate increase in computational expense, the Si(111)-2×1 Pandey π-bonded chain and the Si(111)-2×2 surface reconstructions would provide further insight into the effect of bond breaking and adatom formation on crack surface reconstructions. These would be fruitful subjects for future work, but are beyond the scope of our current study.

Although not the primary thrust of this paper, our calculations are directly applicable to the case of contact between clean Si(100)-2×1 surfaces such as might occur during silicon wafer manufacturing. Si(100)-2×1 is also being considered as a template to self-assemble organic/semiconductor nanostructures,[27] a spatial regime where small energy differences can have enormous effects. Therefore, understanding healing/sticking of surfaces that may occur during manufacturing conditions could have practical implications. Our model omits the effect of mismatched orientation or kinetic effects that arise from the relative motion of the two surfaces. However, as we shall see, it does point to the need to consider the reconstructed surfaces and provides an estimate of the strength of the defective interface.

Two sets of initial conditions were employed to generate the introduced separation (i.e., the "crack" width, denoted by δ and measured relative to the bulk equilibrium interlayer spacing) versus the energy $[\phi(\delta)]$. In the case where the two exposed surfaces are far apart (in practice, 10 Å is sufficient), the energy is two times the relaxed surface energy, $\gamma_r=(\phi(\infty)-\phi(0))/(2A)$, where A is the surface area. The first series of calculations introduced a separation of length δ between two bulk-terminated atomic layers, fixed the unit cell,[28] and allowed all the ionic positions to relax to their minimum-energy configuration. There are two possible outcomes. Either the crack heals, forming a strained bulk crystal, or the crack remains, forming two reconstructed surfaces. The introduced separation could also be thought of as imposed macroscopic deformation or equivalently, a strain. The question is how the deformation is distributed in the material. As Jarvis *et al.*[29] showed, the outcome depends on whether the surfaces are close enough to each other to feel the effects of the electron density on the opposite surface. In essence, the crack can only heal if the two sides can "see" each other. Conceptually, the first scenario is equivalent to either perfectly healing a crack where the surfaces have not had enough time to reconstruct, or forming the first crack from the pristine bulk crystal as it expands under tension. A second series of Si(100) calculations started from the 2×1 reconstructed surfaces known to form on Si(100),[30] sequentially decreased the introduced separation, using the relaxed configuration from the previous step as the initial configuration. Conceptually, this explores how a crack, with reconstructed surfaces, heals. The latter case corresponds to the compression part of fatigue cycling.

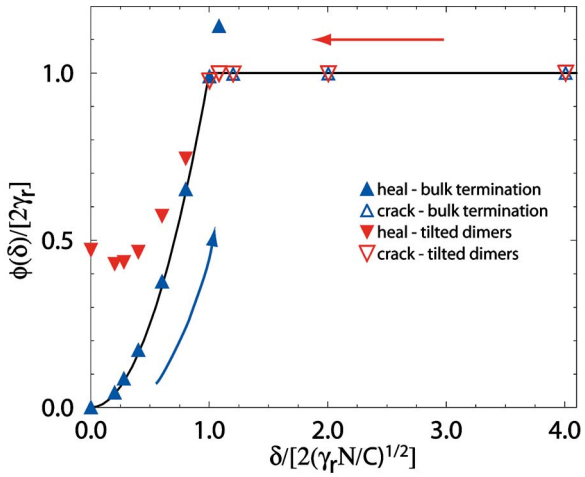

FIG. 1. Normalized energy vs normalized introduced crack widths in silicon along the [001] direction, from DFT calculations. The energy, $\phi(\delta)$, is normalized by $2\gamma_r$ and the introduced crack width, δ, by $\delta/(2\sqrt{\gamma_r N/C})$, according to the universal renormalization (Ref. 35) procedure introduced by Hayes *et al.* (Ref. 31). Two series of calculations were performed. The first started with the ideal bulk termination (blue △) and the second started with the reconstructed surface (red ▽). Cracks that remained after ion relaxation are denoted with open triangles, those that healed are denoted with filled triangles. The arrows indicate cyclic loading of tensile (blue arrow) followed by compressive (red arrow) loads. After the surface reconstructs, the equilibrium bulk crystal cannot be recovered when the crack attempts to heal.

III. RESULTS AND DISCUSSION

Hayes *et al.*[31] recently demonstrated that the energy versus separation curves for metals, semiconductors, and ceramics can all be collapsed to a universal curve if the energy $[\phi(\delta)]$ is normalized by $2\gamma_r$ and if the introduced separation is normalized by $\delta/(2\sqrt{\gamma_r N/C})$, where N is the number of atomic layers in a grain and C is the uniaxial elastic modulus. In order to highlight the universal behavior during the initial cracking and the deviations that arise during subsequent cycles after the crack forms, the results from the DFT calculations are plotted using the normalized variables in Fig. 1. In general, the region below 1.0 in the normalized separation corresponds to a strained bulk configuration, while the region greater than 1.0 corresponds to a cracked configuration.

During fatigue cycling, the following idealized steps occur. At first, there are no cracks so the silicon uniformly expands along the curve with the solid blue upright triangles (▲). Once a critical tension is reached, the bulk crystal becomes unstable and a crack forms, represented by the open blue upright triangles (△) that start at about normalized $\delta=1.0$. Although it is energetically favorable to form a crack with reconstructed surfaces at a normalized separation of 1.1, the crack chooses to form a strained bulk crystal if the calculation is started with the surface atoms at their bulk positions. This demonstrates that there is a small energy barrier separating the equilibrium bulk and reconstructed surface atomic positions. In actual experiments, the transition point will be sensitive to the temperature.

As expected, the initial configuration does not matter once the reconstructed surface forms in the region where the normalized separation is greater than 1.0 (open blue upright triangles, △, and open red down triangles, ▽). In essence, the two surfaces are sufficiently separated so that they can be considered isolated. Since they have no neighbor to please, they do what is best for themselves—in this case that means forming a reconstructed surface. However, the story changes when the compressive portion of the fatigue cycle reaches the region around 1.0. Although it is energetically favorable to form a strained cubic diamond lattice, the crack remains because of the barrier between the reconstructed surface positions and the ideal bulk positions. This effect is more pronounced for silicon compared to metallic systems because of the highly directional nature of its covalent bonds. This has two consequences. First, the crack remains open at lower strains. Second, the healed bulk no longer is a perfect crystal, but rather contains defects along the crack interface. Figure 2 shows the atomic positions (a) and electron density (b,c,d) at the minimum-energy configuration of the healed crack interface for three revealing orientations. In Fig. 2(b), the *yz* plane contains the silicon atoms that were previously reconstructed surface dimers. Figure 2(c) shows the maximum electron density in the *xz* plane between atoms along the healed interface. In Fig. 2(d), the *xy* plane intersects atoms that were on the crack surface before the interface was healed. The electron density between atoms along the healed interface in Figs. 2(b) and 2(d) reveal that the dimer bonds between surface atoms remain, even when the crack is closed. Furthermore, a new bond has formed across the interface as shown by the high (yellow) electron density in the interfacial region in Fig. 2(c). The ideal cubic diamond structure in Fig. 2(b) should be a zigzag pattern like the region away from the interface, but the surface dimer bonds trap the atoms, preventing the crack interface from healing properly. As a consequence, the close proximity of atoms across the interface, relative to the perfect zigzag configuration, cause the minimum-energy configuration to correspond to a structure where the two crack surfaces are farther apart than in the pristine bulk. Dislocations along the interface of a healed crack have been observed experimentally in silicon as early as 1980.[13] These defects are expected to have a significant impact on the strength of the material, as strongly suggested by the solid red down triangles (▽) in Fig. 1. The minimum-energy configuration occurs at a finite positive strain (normalized separation $=\sim 0.2\% \rightarrow \sim 3\%$ strain) and decreases the fracture energy (2γ) by nearly half ($1.13\ \mathrm{J/m^2}$) relative to the equilibrium bulk configuration.

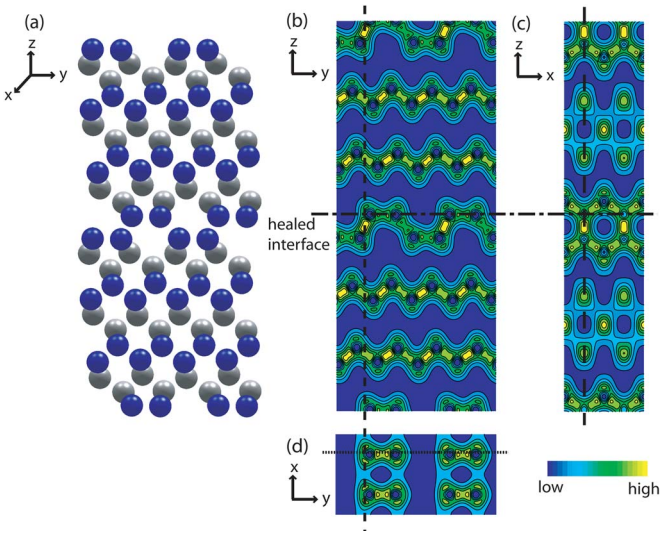

FIG. 2. Electron density plots of the minimum-energy configuration for the healed crack. The *z* direction is doubled so that the healed interface is located just below the dot-dashed line and at the top and bottom (the latter due to periodic boundary conditions). High (low) electron density is denoted in yellow (blue). There is no electron density at the center of the atom due to the use of pseudopotentials. (a) The atomic positions of silicon within a 1×4, 24 layer periodic cell. The blue and silver atoms are on different *yz* planes. (b) The *yz* plane [slice taken at the long dashed line in (c) and dotted line in (d)] contains a dimer of blue atoms from (a) that had formed on the surface before crack healing. (c) The *xz* plane [slice taken at the short dashed line in (b) and (d)] intersects the highest-density region in the healed interface. (d) The 2×4 *xy* plane [slice taken at the dash-dot line in (b) and (c)] intersects the top layer of atoms previously on the crack surface. The electron density between adjacent atoms in the interface layers in (b) and (d) show that the surface dimers remain bonded when the crack is healed. The nearly on-top configuration of atoms across the interface prevents the surfaces from approaching more closely and alters the bonding [see (c)] from the ideal bulk case.

Experimental conditions differ fairly significantly from the idealized case studied here. Temperature, sharp cracks as opposed to two parallel surfaces, crack propagation along the {110} and {111} planes,[24] dynamical effects, and oxide formation due to environmental oxygen and water may all alter the behavior of fatigued cubic diamond silicon. The quantitative numbers and detailed defect structures will most likely differ considerably when compared to experiment. A quantitative theoretical study should employ first-principles molecular dynamics using the correct crack tip geometry and the (111)Si crack surface for at least one complete fatigue cycle, which is computationally prohibitive at present. What our study does do is to isolate the role that surface bond formation plays in crack formation and healing during fatigue cycling in systems which exhibit surface reconstruction due to strong covalent bonds. The qualitative picture that arises is a flawed, healed crack interface that should be both weaker and more strained than would be expected based on the perfect crystal. The weakened interface may be susceptible to adatom migration, bond rearrangement, or oxidation in subsequent tensile/compressive cycles, especially at elevated temperatures. This supports the theory that mechanically induced subcritical cracking can greatly weaken silicon

by introducing irreversible damage via strong directional bond formation, eventually leading to fatigue failure. Moreover, the extra strain introduced into the system in the crack tip region due to the interfacial defects arising from imperfect crack healing may also make the system more vulnerable to oxide formation, further accelerating the failure process by either oxide dissolution or stress corrosion cracking.

ACKNOWLEDGMENTS

This work was supported by a Department of Defense-MURI grant through Brown University's MURI Center for the "Design and Testing of Materials by Computation: A Multi-Scale Approach" and the U.S. Air Force Office of Scientific Research. One of the authors (R.L.H.) thanks the National Defense Science and Engineering Graduate Fellowship for funding.

[1] J. A. Connally and S. B. Brown, Science **256**, 1537 (1992).
[2] P. Shrotriya, S. M. Allameh, S. B Brown, Z. Suo, and W. O. Soboyejo, Exp. Mech. **50**, 289 (2003).
[3] C. L. Muhlstein, E. A. Stach, and R. O. Ritchie, Acta Mater. **50**, 3579 (2002).
[4] H. Kahn, R. Ballarini, J. Bellante, and A. H. Heuer, Science **298**, 1215 (2002).
[5] E. D. Renuart, A. M. Fitzgerald, T. W. Kenny, and R. H. Dauskardt, J. Mater. Res. **19**, 2635 (2004).
[6] H. Kahn, R. Ballarini, and A. H. Heuer, Curr. Opin. Solid State Mater. Sci. **8**, 71 (2004).
[7] M. C. Flowers, N. B. H. Jonathan, A. Morris, and S. Wright, Surf. Sci. **351**, 87 (1996).
[8] S. Ogata, F. Shimojo, R. K. Kalia, A. Nakano, and P. Vashishta, J. Appl. Phys. **95**, 5316 (2004).
[9] R. Belkada, T. Igarashi, and S. Ogata, Comput. Mater. Sci. **30**, 195 (2004).
[10] W. WongNg, G. S. White, S. W. Freiman, and C. G. Lindsay, Comput. Mater. Sci. **6**, 63 (1996).
[11] R. K. Kalia, A. Nakano, P. Vashishta, C. L. Rountree, L. Van Brutzel, and S. Ogata, Int. J. Fract. **121**, 71 (2003).
[12] A. M. Fitzgerald, R. S. Iyer, R. H. Dauskardt, and T. W. Kenny, J. Mater. Res. **17**, 683 (2002).
[13] B. R. Lawn, B. J. Hockey, and S. M. Wiederhorn, J. Mater. Sci. **15**, 1207 (1980).
[14] D. G. Li, N. S. McAlpine, and D. Haneman, Appl. Surf. Sci. **65–66**, 553 (1993).
[15] D. Haneman, N. S. McAlpine, E. Busch, and C. Kaalund, Appl. Surf. Sci. **92**, 484 (1996).
[16] L. A. Marqués, L. Pelaz, J. Hernández, J. Barbolla, and G. H. Gilmer, J. Phys. Chem. **64**, 045214 (2001).
[17] K. Yasutake, M. Iwata, K. Yoshii, M. Umeno, and H. Kawabe, J. Mater. Sci. **21**, 2185 (1986).
[18] J. C. H. Spence, Y. M. Huang, and O. Sankey, Acta Metall. Mater. **41**, 2815 (1993).
[19] R. Perez and P. Gumbsch, Phys. Rev. Lett. **84**, 5347 (2000).
[20] N. Bernstein and D. W. Hess, Phys. Rev. Lett. **91**, 025501 (2003).
[21] T. Hoshi and T. Fujiwara, J. Phys. Soc. Jpn. **72**, 2429 (2003).
[22] J. P. Perdew and Y. Wang, Phys. Rev. B **45**, 13244 (1992).
[23] G. Kresse and J. Furthmüller, Comput. Mater. Sci. **6**, 15 (1996).
[24] D. Sherman and I. Beéry, J. Mech. Phys. Solids **52**, 1743 (2004).
[25] P. Minary, M. E. Tuckerman, K. A. Pihakari, and G. J. Martyna, J. Chem. Phys. **116**, 5351 (2002).
[26] K. Shimada, T. Ishimaru, T. Watanabe, T. Yamawaki, M. Osuka, T. Hoshino, and I. Ohdomari, Phys. Rev. B **62**, 2546 (2000).
[27] M. C. Hersam and R. G. Reifenberger, MRS Bull. **29**, 385 (2004).
[28] The unit cell is "fixed" in the directions parallel to the "crack" at the equilibrium lattice constant A_{eq}, while in the direction perpendicular to the incipient crack, the lattice constant is given by $A_{eq}+\delta$.
[29] E. A. A. Jarvis, R. L. Hayes, and E. A. Carter, ChemPhysChem **2**, 55 (2001).
[30] H. Over, J. Wasserfall, W. Ranke, C. Ambiatello, R. Sawitzki, D. Wolf, and W. Moritz, Phys. Rev. B **55**, 4731 (1997).
[31] R. L. Hayes, M. Ortiz, and E. A. Carter, Phys. Rev. B **69**, 172104 (2004).
[32] *CRC Handbook of Chemistry and Physics*, 84th ed., edited by D. R. Lide (CRC, Boca Raton, FL, 2004).
[33] G. Simmons and H. Wang, *Single Crystal Elastic Constants and Calculated Aggregate Properties: A Handbook*, 2nd ed. (MIT, Cambridge, MA, 1971).
[34] D. J. Eaglesham, L. C. White, A. E. Feldman, N. Moriya, and D. C. Jacobson, Phys. Rev. Lett. **70**, 1643 (1993).
[35] O. Nguyen and M. Ortiz, J. Mech. Phys. Solids **50**, 1727 (2002).